2018

Assessment of Antarctic moss health from multi-sensor UAS imagery with Random Forest Modelling

Darren Turner
University of Tasmania

Arko Lucieer
University of Tasmania, arko.lucieer@utas.edu.au

Zbynek Malenovky
University of Wollongong, zbynek@uow.edu.au

Diana H. King
University of Wollongong, dhk442@uowmail.edu.au

Sharon A. Robinson
University of Wollongong, sharonr@uow.edu.au

Assessment of Antarctic moss health from multi-sensor UAS imagery with Random Forest Modelling

Abstract

Moss beds are one of very few terrestrial vegetation types that can be found on the Antarctic continent and as such mapping their extent and monitoring their health is important to environmental managers. Across Antarctica, moss beds are experiencing changes in health as their environment changes. As Antarctic moss beds are spatially fragmented with relatively small extent they require very high resolution remotely sensed imagery to monitor their distribution and dynamics. This study demonstrates that multi-sensor imagery collected by an Unmanned Aircraft System (UAS) provides a novel data source for assessment of moss health. In this study, we train a Random Forest Regression Model (RFM) with long-term field quadrats at a study site in the Windmill Islands, East Antarctica and apply it to UAS RGB and 6-band multispectral imagery, derived vegetation indices, 3D topographic data, and thermal imagery to predict moss health. Our results suggest that moss health, expressed as a percentage between 0 and 100% healthy, can be estimated with a root mean squared error (RMSE) between 7 and 12%. The RFM also quantifies the importance of input variables for moss health estimation showing the multispectral sensor data was important for accurate health prediction, such information being essential for planning future field investigations. The RFM was applied to the entire moss bed, providing an extrapolation of the health assessment across a larger spatial area. With further validation the resulting maps could be used for change detection of moss health across multiple sites and seasons.

Disciplines

Medicine and Health Sciences | Social and Behavioral Sciences

Publication Details

Turner, D., Lucieer, A., Malenovsky, Z., King, D. & Robinson, S. A. (2018). Assessment of Antarctic moss health from multi-sensor UAS imagery with Random Forest Modelling. International Journal of Applied Earth Observation and Geoinformation, 68 168-179.

Title

Assessment of Antarctic Moss Health from Multi-sensor UAS Imagery with Random Forest Modelling

Authors

Darren Turner*[1] – Darren.Turner@utas.edu.au

Arko Lucieer[1] – Arko.Lucieer@utas.edu.au

Zbyněk Malenovský[1 2 3] - zbynek.malenovsky@gmail.com

Diana King[2] - dhk442@uowmail.edu.au

Sharon A. Robinson[2] - sharonr@uow.edu.au

*Corresponding author

[1] School of Land and Food, University of Tasmania, Sandy Bay, Tasmania, 7005, Australia

[2] Australia Centre for Sustainable Ecosystem Solutions, School of Biological Sciences, University of Wollongong, NSW 2522, Australia

[3] Department of Remote Sensing, Global Change Research Institute CAS, Bělidla 986/4a, CZ-60300 Brno, Czech Republic

Keywords

UAV; UAS: Random Forest Models; Antarctica; Moss; Multispectral; Visible; Thermal; Digital Surface Model

Abstract

Moss beds are one of very few terrestrial vegetation types that can be found on the Antarctic continent and as such mapping their extent and monitoring their health is important to environmental managers. Across Antarctica, moss beds are experiencing changes in health as their environment changes. As Antarctic moss beds are spatially fragmented with relatively small extent they require very high resolution remotely sensed imagery to monitor their distribution and

dynamics. This study demonstrates that multi-sensor imagery collected by an Unmanned Aircraft System (UAS) provides a novel data source for assessment of moss health. In this study, we train a Random Forest Regression Model (RFM) with long-term field quadrats at a study site in the Windmill Islands, East Antarctica and apply it to UAS RGB and 6-band multispectral imagery, derived vegetation indices, 3D topographic data, and thermal imagery to predict moss health. Our results suggest that moss health, expressed as a percentage between 0 and 100% healthy, can be estimated with a root mean squared error (RMSE) between 7 and 12%. The RFM also quantifies the importance of input variables for moss health estimation showing the multispectral sensor data was important for accurate health prediction, such information being essential for planning future field investigations. The RFM was applied to the entire moss bed, providing an extrapolation of the health assessment across a larger spatial area. With further validation the resulting maps could be used for change detection of moss health across multiple sites and seasons.

1. Introduction

The health of moss beds in Antarctica is of scientific interest due to their sensitivity to climate change. Several studies have investigated their response to dynamic climatic conditions (Amesbury et al., 2017; Casanovas et al., 2015; Clarke et al., 2012; Convey et al., 2009; Dunn and Robinson, 2006; Robinson et al., 2003; Turnbull and Robinson, 2009). The growth and health of these moss beds is highly reliant on environmental factors, particularly availability of liquid water and sufficient nutrient supply, typically originating from guano in ancient penguin rookeries (Melick et al., 1994; Wasley et al., 2012). While the Windmill Islands region of East Antarctica contains some of the most extensive vegetation communities found in the Antarctic region (Smith, 1988), these moss beds are of limited extent (< 1 ha) and highly spatially fragmented. Their complex topography, combined with the isolation of the site, generally create a challenge for spatial monitoring of community change (Convey et al., 2014). In our previous studies, we have demonstrated that Unmanned Aircraft Systems (UAS), also known as Unmanned Aerial Vehicles (UAVs) or drones, provide an excellent tool for mapping these areas (Lucieer et al., 2014b; Malenovský et al., 2017; Turner et al., 2014a). The advantage of UAS, combined with imaging spectroscopy and other optical observations, is that it allows mapping of moss health over large areas relatively quickly, non-destructively and on demand under clear sky or overcast conditions (Malenovský et al., 2017; Malenovský et al., 2015).

The use of high resolution remote sensing techniques for mapping the spatial patterns and dynamics of Antarctic vegetation is relatively limited. The concept of mapping Antarctic moss beds was first introduced by Lucieer et al. (2011) and Lucieer et al. (2012). A relationship between water availability and moss health was then found by Lucieer et al. (2014b) but unlike our current study a

continuous map of moss health was not produced. Relating moss health to the MTVI vegetation index (Turner et al., 2014a) allowed the first thematic maps of moss health to be produced. Lucieer et al. (2014a) first introduced the concept of using hyperspectral imaging to map moss vigour, followed by Malenovský et al. (2017) who used hyperspectral data to map moss chlorophyll content and leaf density. The spatial extent of cyanobacterial mats has also been mapped in the dry valleys of Antarctica using a fixed wing UAS that covered a large area (> 10 ha) (Bollard-Breen et al., 2014).

Whilst we have demonstrated that spatially accurate, multi-sensor data can be collected over Antarctic moss beds with a small UAS (Lucieer et al., 2014b; Turner et al., 2014a), we have not yet identified the optimal combination of sensors and spectral bands from these multi-sensor data for the extraction of biophysical derivatives, such as moss health. This study addresses this gap by assessing moss health from multi-sensor UAS data – RGB, multispectral, 3D terrain, and thermal – and identifying the sensors and variables that contribute most to this assessment.

Random Forest Models (RFMs) were first introduced by Breiman (2001) and their application in remote sensing for classification and regression has grown rapidly. A common use for RFMs is to classify spectral satellite images. For example Eisavi et al. (2015) and Zhu (2013) tested the ability of RFMs to classify Landsat ETM images into land cover classes and reported overall accuracies of up to 90% and 82%, respectively. Higher spatial resolution satellite imagery was used to detect landslides with a combination of Object Based Image Analysis (OBIA) and RFMs by Stumpf and Kerle (2011), who reported an overall accuracy of up to 87%. Rather than classifying the input data into discrete classes, RFMs are also capable of a regression analysis estimating quantitative variables, typically related to a biogeophysical or biogeochemical measurement of the environment. For example Wang et al. (2016) used high resolution satellite data and an RFM to estimate the biomass of wheat crops. The application of RFMs is not only restricted to satellite imagery. Yuan and Hu (2016) used features of visible UAS imagery, segmented it with OBIA, to train an RFM in detection of forest pests. Feng et al. (2015) pre-processed UAS imagery by calculating texture measures and trained an RFM to classify urban vegetation with an overall accuracy of up to 90%.

Our previous research (Turner et al., 2014a) focused on the co-registration of various images of Antarctic moss beds acquired with multiple off-the-shelf sensors carried by small-size UAS. The aim of this study is to apply RFMs to this multi-sensor UAS dataset to assess actual moss health. RFMs are said to be particularly powerful when analysing many weak explanatory variables, i.e. in cases when no single variable, or group of variables, is able to estimate the expected output (Breiman, 2001). Another strong feature of RFMs is the capability to provide a measure of variable importance, i.e. a measure of how much each of the input variables contributed to the RFM prediction. This information can be used to reduce the number of input variables in an attempt to improve the

performance and simplify computational complexity of the RFM (Millard and Richardson, 2015). The measure of variable prediction power provides the ability to experiment with the removal of one or multiple sensors from the input dataset, in a similar manner to Corcoran et al. (2013). Identifying the most optimal combination of input datasets would allow optimal collection of UAS data, which in turn makes fieldwork more efficient and cost-effective. This is of particular importance in Antarctica where fieldwork time is limited and low temperatures adversely affect sensors and degrade battery performance.

This study investigates the optimal approach to train and validate an RFM with data from multi-sensor UAS imagery (RGB colour photographs, 6-band multispectral and broadband thermal images) to predict the health of Antarctic moss beds based on ground observations collected in the field and analysed in the lab (Ashcroft et al., 2016; Ashcroft et al., 2017; Wasley et al., 2012).

2. Methodology

2.1 Field sites

We collected UAS imagery at the Robinson Ridge study site in the Windmill Islands region, East Antarctica on 24th February 2011 and on 3rd February 2014. This site, which contains some of the best moss beds in the region, has been part of a long-term monitoring program assessing community health since 2000 (Robinson and King, 2017 pers.comm., 31 Oct; Wasley et al., 2012). The site is located approximately 10 km south of the Australian Antarctic station Casey (see Figure 1). The study area has been extensively described in Lovelock and Robinson (2002), Dunn and Robinson (2006), Turner et al. (2012), Lucieer et al. (2014b), and Turner et al. (2014a).. Due to sensor availability and protocol changes, there were some differences between the data collected in 2011 and 2014.

There are numerous challenges associated with collecting field data in Antarctica, and in particular when deploying a UAS with multiple sensors. Initially, there are the logistical hurdles of getting personnel and equipment to the field site. The summer growing season for the moss is very short, sometimes only a matter of weeks if the thaw is delayed (Dunn and Robinson, 2006). Even during the growing season, there can be periods of bad weather that result in the moss beds being temporarily covered in snow making optical remote sensing impossible. The low temperatures experienced on most days (-10 °C – 0 °C) cause difficulties for the sensors and UAS airframes, in particular the batteries which do not perform well in the cold and thus reduce UAS flight duration. Finally, once on site with snow-free moss beds the weather conditions on the day need to be

suitable for both UAS operations (low wind speeds) and data collection (sufficiently high solar irradiance).

In 2014, logistical issues such as those described meant that time at the Robinson Ridge field site was limited and not all sensors were available. This resulted in limited spatial coverage of the study area by the UAS flight (see Figure 1 where the red outline denotes the extent of UAS data collection). The reduction in spatial coverage in 2014 meant fewer ground validation plots were covered.

Figure 1 – Site location map of the Robinson Ridge field site within the Windmill Islands, East Antarctica. Imagery is from RGB sensor flight in 2011.Coloured boxes show locations of the long-term monitoring quadrats, Green markers - Bryophyte quadrats, Orange markers -Transitional quadrats. Red outline indicates extent of 2014 data aerial collection. Drainage channels run NNW from the snow bank on the eastern side down the slope towards the sea.

2.2 UAS Platform

This study made use of a Mikrokopter UAS called an 'Oktokopter' supplied by HiSystems (GmbH, www.mikrokopter.com, Germany) (see Figure 2). The Oktokopter has a flight duration of approximately 5 mins when carrying a typical payload of around 1 kg. The flight duration was shortened slightly by the cold environment (approx. -10 °C), however, the main problem for the batteries was keeping them warm before they were used. When the battery is cold (close to freezing temperatures) the chemical reaction within the battery is unable to provide sufficient power for safe flight. We kept the batteries warm (approx. 15 °C) in the field by storing them in an insulated box with a heating source. Since the time of data collection both airframe and battery technology have improved, thus it would now be feasible for a modern multi-rotor UAS to fly with a similar payload for up to 30 minutes. The Oktokopter uses a gimballed camera mount to keep the sensor pointed at nadir during flight operations. The electronics systems on-board the UAS are used to maintain level flight, to log system data, and to fly the UAS through a series of predefined waypoints.

Figure 2 - Oktokopter fitted with Tetracam mini-MCA 6 band multispectral camera

2.3 Sensors

Three sensors were used to investigate moss health: i) an RGB camera Canon 550D DSLR (15 Megapixel, 5184 x 3456 pixels, with Canon EF-S 18-55 mm F/3.5-5.6 IS lens), ii) a multispectral camera Tetracam (Tetracam, Inc., USA) -6-band mini-MCA (Multiple Camera Array), and iii) a thermal infrared camera FLIR Photon 320 (FLIR Systems, Inc., the USA, www.flir.com). Further details about the sensors can be found in Turner et al. (2014a) and Lucieer et al. (2014b). Due to the payload

weight limit of the UAS platform, each sensor was carried on a separate flight. Data from the three sensors was co-registered based on the workflow described in Turner et al. (2014a).

The raw data from the thermal sensor was calibrated to ground surface temperature by means of an empirical line correction that used nineteen ground measurements taken with a thermal radiance gun (Digitech QM7226). A linear regression was calculated to establish a relationship between the reference temperature measurements and raw DN values of thermal single band imagery at coincident sites. This relationship was applied per pixel to convert the whole thermal image into absolute temperature values; further details can be found in Turner et al. (2014a).

Mosaics of multispectral images were also converted from raw DN values to physically meaningful reflectance values with an empirical line correction (Smith and Milton, 1999). Spectral calibration targets, producing uniform near-Lambertian reflectance signatures, were placed in the study area during the flights (three targets for 2011 dataset and five targets for 2014 dataset). The reflectance functions of the panels were measured on the ground with an ASD HandHeld2 spectroradiometer (Analytical Spectral Devices, PANalytical Boulder USA) and empirically related to the DN values for the same panels in the imagery (Lucieer et al., 2014b). The established empirical line correction was then applied to the whole image dataset to standardise the multispectral signal as the relative reflectance function.

2.4 Moss health ground validation data

Since the primary purpose of this study is to map moss health, availability of sufficient and accurate ground truth data is imperative. Thirty vegetation quadrats (see Figure 3) were established within the Robinson Ridge study area in 2003 as part of a long-term monitoring system for Australian State of the Environment Indicator 72 (SoE 72, https://data.aad.gov.au/aadc/soe/display_indicator.cfm?soe_id=72). The quadrats encompass three community types (ten of each): Bryophyte, Transitional (in-between) and Lichen dominated, which generally reflect the gradient from wettest to drier areas, respectively (see Figure 1) (Wasley et al., 2012). The quadrats are located by way of permanent markers attached to adjacent rocks and have been monitored at least every five years since 2003. To quantify the health of the moss in a quadrat, 9 small samples of moss were taken on a 3 by 3 central grid within each 25 x 25 cm quadrat and returned to the lab for further analysis. The species composition and physiological status of the sampled shoots (i.e. healthy or moribund) were used to calculate an overall health per quadrat as a percentage. Further details on the moss monitoring methodology can be found in Wasley et al. (2012), Lucieer et al. (2014b) and (Robinson and King, 2017 pers. comm. 31 Oct). For this study, we only used the Bryophyte and Transitional quadrats (Figure 1), as distinguishing vegetation from the

surrounding rocks and soil in the UAS imagery of the Lichen quadrats was unreliable. Lichen is a completely different organism to moss and not easy to discriminate from the spectrally similar rock surfaces, thus the lichen quadrats we not used and considered to be outside the scope of this study.

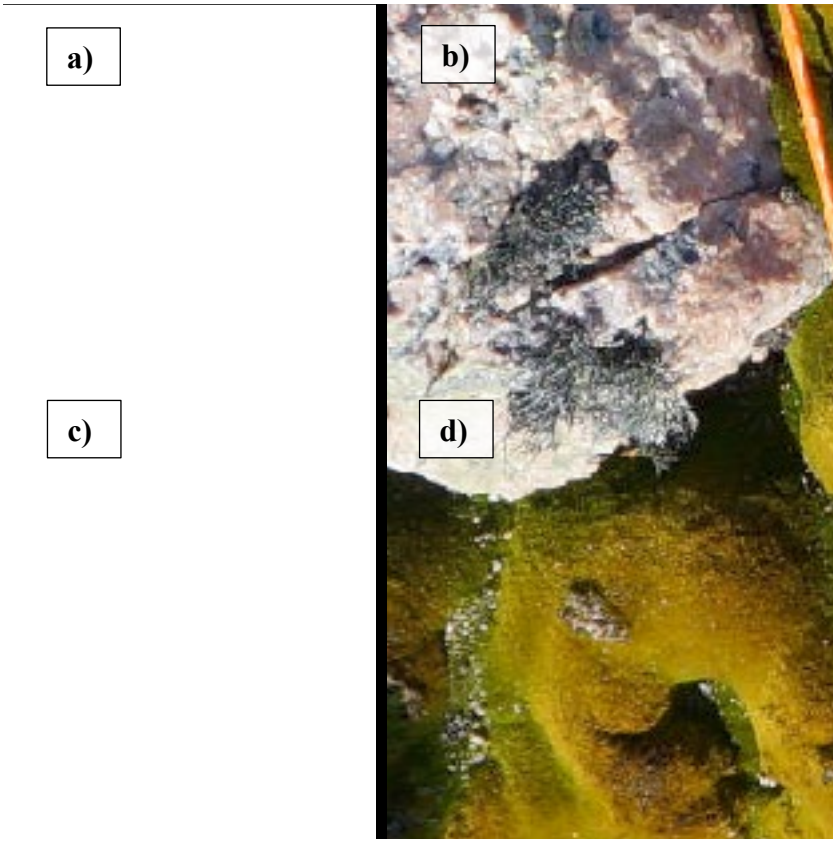

Figure 3 – Example of a moss quadrat a) ground based photo showing permanent marker on rock and temporary quadrat frame (25 x 25 cm), b) high resolution (1 cm/pixel) UAS RGB image, c) medium resolution (3 cm/pixel) false colour multispectral UAS image , d) low resolution (10 cm/pixel) thermal UAS image

2.5 Orthophoto creation

For each UAS flight, involving a different sensor, hundreds of images are collected. Image data from each sensor requires georeferencing, and, where necessary, calibration, before creating the orthomosaic map. Each orthomosaic must be accurately georeferenced such that data from each sensor can be superimposed, i.e. when information is extracted from one sensor orthomosaic then it originates from the same location in all the other orthomosaics and their derivatives.

Orthomosaic generation for the visible and thermal imagery made use of the structure-from-motion (SfM) workflow in Photoscan, which is a well-established software package for processing overlapping imagery captured by a UAS (Immerzeel et al., 2014; Javernick et al., 2014; Turner et al., 2014b; Verhoeven, 2011). Nevertheless, for our multispectral imagery the Photoscan workflow did not work as expected, most likely due to rolling shutter effects of the multispectral sensor. Therefore, we implemented a new technique that made use of a Scale Invariant Feature Transform

(SIFT) to detect features within each multispectral frame and match them with features detected in the already georeferenced visible orthophoto. The matched features were then used as control points to warp each multispectral frame into the same co-ordinate system as the visible imagery as described in Turner et al. (2014a).

2.6 Random Forest Model input variables

In this study, we trained several RFMs with a set of input variables derived from the multi-sensor UAS imagery with the objective to predict moss health as the independent variable. Breiman (2001) states that an RFM model is particularly powerful when working with many weak explanatory variables, where the output cannot be distinguished by any single variable or limited group of variables. Thus we derived as many model input variables as possible that potentially contributed to the prediction of moss health (see Table 1). From previous studies we know that there is a relationship between MTVI (Turner et al., 2014a), water availability (Lucieer et al., 2014b), and moss health. With this knowledge we selected variables (e.g. terrain-based such a wetness index and skyview factor) that we expected to have an environmental relationship to moss health. Apart from Flow Accumulation, Terrain Wetness Index (TWI), Terrain Roughness Index (TRI), and Skyview, the input variables were extracted from various sensor data with the ENVI software package (Exelis Visual Information Solutions, Inc., USA, www.exelisvis.com). A by-product of the orthophoto generation workflow was a Digital Surface Model (DSM), which was used to model the terrain. The Flow Accumulation was modelled with a Monte Carlo simulation, estimating the snowmelt runoff from upstream of the moss field, as detailed in Lucieer et al. (2014b). Skyview (predicting the potential amount of sunlight received by any given part of the moss bed), TWI (indicating the potential terrain wetness) and TRI (assessing the roughness of the terrain) were all generated with the SAGA software package (Conrad et al., 2015). Skyview factor was modelled with the Skyview factor tool in SAGA using the default maximum search radius and the sector methodology. Both the TWI and the TRI were modelled using the SAGA default parameters. The spectral vegetation indices were based on spectral band calculations in ENVI and then exported as new layers for the RFM training dataset.

Before the training dataset could be extracted from the image layers, it was essential to ensure that layers were accurately co-registered and that accurately measured geo-locations were available for the moss health monitoring quadrats (described in Section 2.4). The accuracy of the co-registration of the datasets was already known to be approximately within 2 pixels for any given layer, see Turner et al. (2014a). Accurate central coordinates for each quadrat were collected with a survey-grade Differential Global Navigation Satellite System (GNSS) receiver (2 – 4 cm absolute accuracy)

during the 2010 field season. Using these coordinates as a starting point, knowing the quadrats are 25 cm x 25 cm, and by using detailed ground photos (similar to Figure 3) the locations of the corners of the quadrats were calculated and then used to digitise a polygon for each quadrat (see Figure 3). The pixel values were extracted from image layers of each polygon to create training and testing data for the RFM, respectively. Each set of pixels from a given polygon was assigned the field measured moss health percentage obtained for the matching ground quadrat. Some quadrats contained areas of rocks and stones, which needed to be filtered out. We found that by applying a threshold of 0.1 to the MTVI map, it was possible to detect and reliably remove the rock pixels from the quadrats.

Table 1 - Variables used as inputs for the Random Forest Model training/testing. Only variables highlighted in grey were available in 2014 dataset

Variable Name(s)	Sensor	Description
R, G, B	Visible	Raw Red, Green, and Blue values from digital camera
H, S, V	Visible	Visible RGB pixels converted into Hue Saturation Value
PC1, PC2, PC3	RGB	Principal Component Analysis of three RGB bands in visible imagery
TWI	Visible (DSM)	Topographic Wetness index as modelled from DSM - (Sørensen et al., 2006)
TRI	Visible (DSM)	Terrain Ruggedness Index as modelled from DSM
Slope	Visible (DSM)	Slope as modelled from DSM
Flow Accumulation	Visible (DSM)	Flow Accumulation as modelled from DSM, see Lucieer et al. (2014b)
Skyview	Visible (DSM)	Skyview as modelled from DSM
$Refl_{530}$	Multispectral	Calibrated surface reflectance for 530nm band
$Refl_{550}$	Multispectral	Calibrated surface reflectance for 550nm band
$Refl_{570}$	Multispectral	Calibrated surface reflectance for 570nm band
$Refl_{670}$	Multispectral	Calibrated surface reflectance for 670nm band
$Refl_{700}$	Multispectral	Calibrated surface reflectance for 700nm band
$Refl_{720}$	Multispectral	Calibrated surface reflectance for 720nm band
$Refl_{750}$	Multispectral	Calibrated surface reflectance for 750nm band
$Refl_{800}$	Multispectral	Calibrated surface reflectance for 800nm band
MTVI2	Multispectral	Modified Triangular Vegetation Index 2 - (Haboudane et al., 2004) $= \frac{1.5[1.2(Refl_{800} - Refl_{550}) - 2.5(Refl_{670} - Refl_{550})]}{\sqrt{(2Refl_{800} + 1)^2 - (6Refl_{800} - 5\sqrt{Refl_{670}}) - 0.5}}$
NDVI	Multispectral	Normalised Difference Vegetation Index - (Tucker, 1979) $NDVI = \frac{Refl_{800} - Refl_{670}}{Refl_{800} + Refl_{670}}$
SR	Multispectral	Simple Ratio Vegetation Index $SR = \frac{Refl_{800}}{Refl_{670}}$
PRI	Multispectral	Photochemical Reflectance Index - (Gamon et al., 1992) $PRI = \frac{Refl_{570} - Refl_{530}}{Refl_{570} + Refl_{530}}$
Surface Temperature	Thermal	Calibrated moss surface temperature as calculated from raw thermal imagery (see Section 2.3)

2.7 Random Forest Model training and testing

We implemented the RFM in the Python programming environment using the Scikit-learn machine learning module (see http://scikit-learn.org/stable/). The first stage of training an RFM is to

determine how many “trees” are required in the RFM to maintain accuracy of the output. The optimal number of trees has been found to vary, the minimum number for a classification RFM was reported to be as few as 100 (Lawrence et al., 2006) up to 300 (Akar and Güngör, 2015), whilst other studies (Corcoran et al., 2013; Lawrence et al., 2006) have found that as many as 500 trees are needed to produce accurate results. Thus to find the optimum, we iteratively adjusted the number of trees and compared the estimated error of the RFM until it had converged.

During the RFM training, the model error can be assessed using the Out of Bag Error estimator (OOBE). The OOBE is considered an independent accuracy assessment (Breiman, 2001). Several studies, such as Lawrence et al. (2006) and Liaw and Wiener (2002), have found the OOBE to be a good indicator of an RFMs accuracy, supporting the assertion that an RFM does not need an independent accuracy assessment. However, in some other studies, such as Millard and Richardson (2015), it was found that the OOBE underestimated the RFM error as compared to the error measured on an independent dataset. They deduced that OOBE was not a good indicator for high dimensional datasets. Other studies have also obtained better assessment of accuracy when a part of the data was reserved for a traditional error assessment (Corcoran et al., 2013). For this study we used the OOBE to monitor the RFM as we changed model parameters, and then used the root mean squared error (RMSE) computed from an independent test dataset to assess the final RFM accuracy. Also, whilst training the RFM, the model was run through 50 iterations to ensure the apparent effects of parameter changes were not just random variations.

In addition to the number of trees, there are a number of other parameters of an RFM that can be adjusted, such as: i) the number of variables to consider when looking for the best split, ii) the maximum depth of the tree, and iii) the minimum number of samples required to be at a leaf node. Boulesteix et al. (2012) suggested that the default value for the number of variables considered for a split (one third of the total number of variables) was too low, especially when the data is noisy. Varying parameters can make the RFM less prone to capturing noise in the training data and for the model to overfit. When building our RFMs, we iteratively adjusted these parameters and assessed their effect on the OOBE.

2.8 Model validation

To finally validate the performance of an RFM we used an independent test dataset, as suggested by Hammond and Verbyla (1996), that was not used for the RFM training. Retaining 20-30% of the input data is a common way to validate the RFM performance (Corcoran et al., 2013). However, to fully validate the RFM, cross-validation of the testing dataset is required, such that different combinations of testing data are examined. Our dataset was not large enough (in terms of total

number of quadrats) to allow a full cross-validation. Therefore, we decided to select 5 of the 20 quadrats (25%) as the test dataset and to test all combinations of test quadrats possible. We trained and validated the model 15504 times based on all combinations of 5 test quadrats and training the RFM with the remaining 15 quadrats, and recorded the RMSE. The mean RMSE for all combinations was used as a summary indicator for model performance.

3. Results

3.1 Number of trees

The first RFM was trained with data for the Robinson Ridge site acquired in 2011. It used the 25 available input variables extracted from the UAS imagery and attempted to model the health for 20 quadrats (Bryophyte and Transitional) as measured in 2011. The effect of the number of RFM trees on the OOBE can be seen in Figure 4a. It suggests that the OOB error converges when approximately 200-300 trees are implemented.

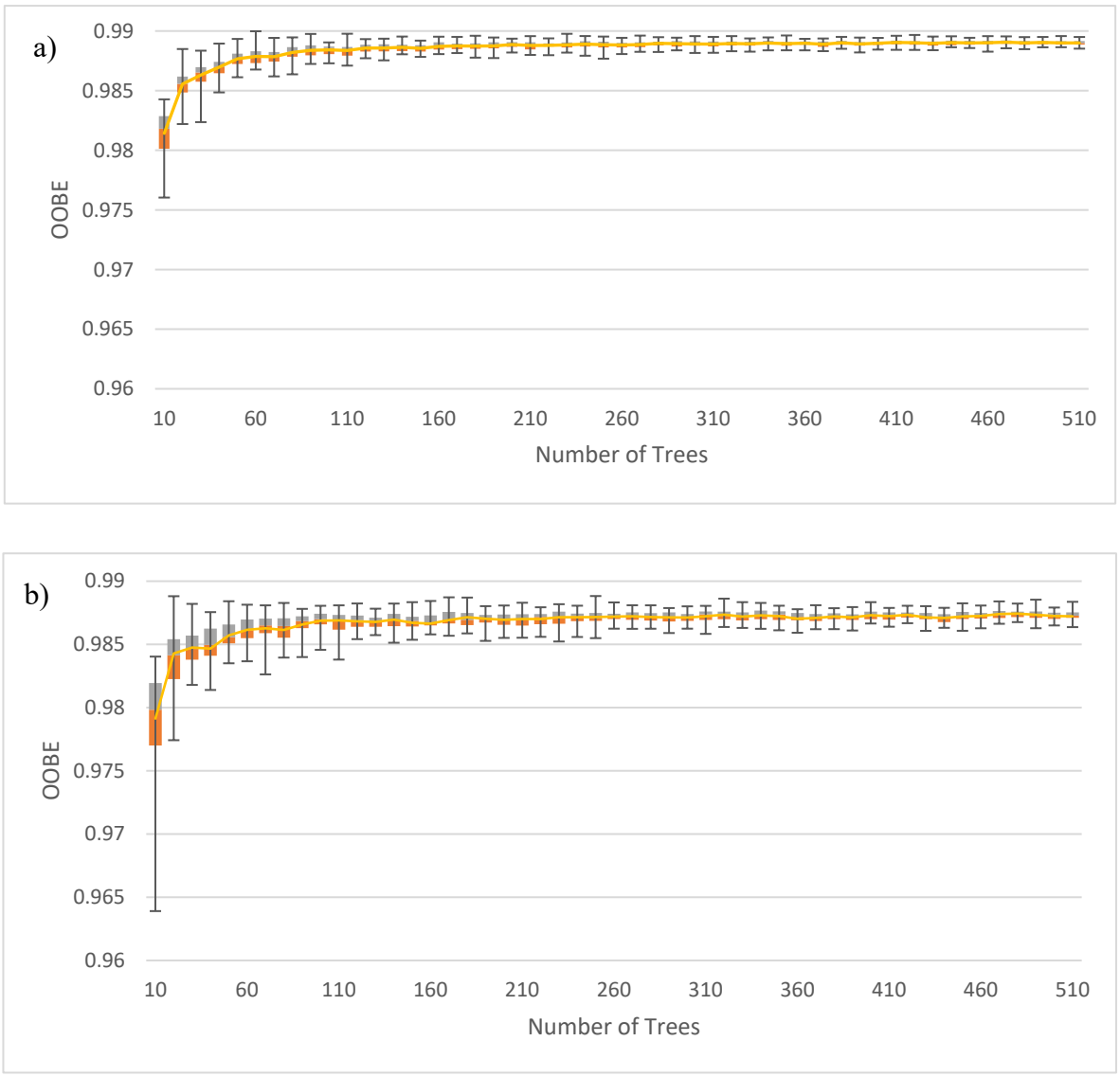

Figure 4 – Optimising number of trees for Robinson Ridge a) 2011 and b) 2014 Random Forest Models. 50 iterations of model were run for every 10 trees. Error bars indicate maximum/minimum values. Boxes show quartile values.

The second model was trained for the Robinson Ridge 2014 dataset. Due to availability and logistical constraints, not all the sensors were deployed in 2014, reducing the number of input variables to 14. Since only a part of the research area was flown, recorded UAS data did not cover all the ground quadrats. In addition, some quadrats were flooded by melt water at the time of data collection. As a result, there were only 5 bryophyte and 3 transitional quadrats available as testing/training data, the 2014 model converged when approximately 200-300 trees are implemented, as was the case for the 2011 model (see Figure 4b).

3.2 Other Random Forest Model parameters

Another RFM parameter (max_features) specifies the number of input variables that are considered at each split. By default this parameter is set to use all variables. Reducing the number of features can improve RFM performance, especially if the data is too noisy (Boulesteix et al., 2012), and perhaps reduce the chance that the RFM will overfit the training data. Liaw and Wiener (2002) suggested that this parameter should not be set to the default, in particular for a regression-based RFM. The results of varying this parameter can be seen in Figure 5. It demonstrates that a lower (non-default) value produces better results, supporting the suggestion that a small number of features reduces the chance of the RFM overfitting. Adjustment of other parameters, such as the maximum depth of the tree (max_depth) and the minimum number of samples required to be at a leaf node (min_samples_leaf), was also tested. Since no effect on the RFM performance was found, these parameters were left at their default settings.

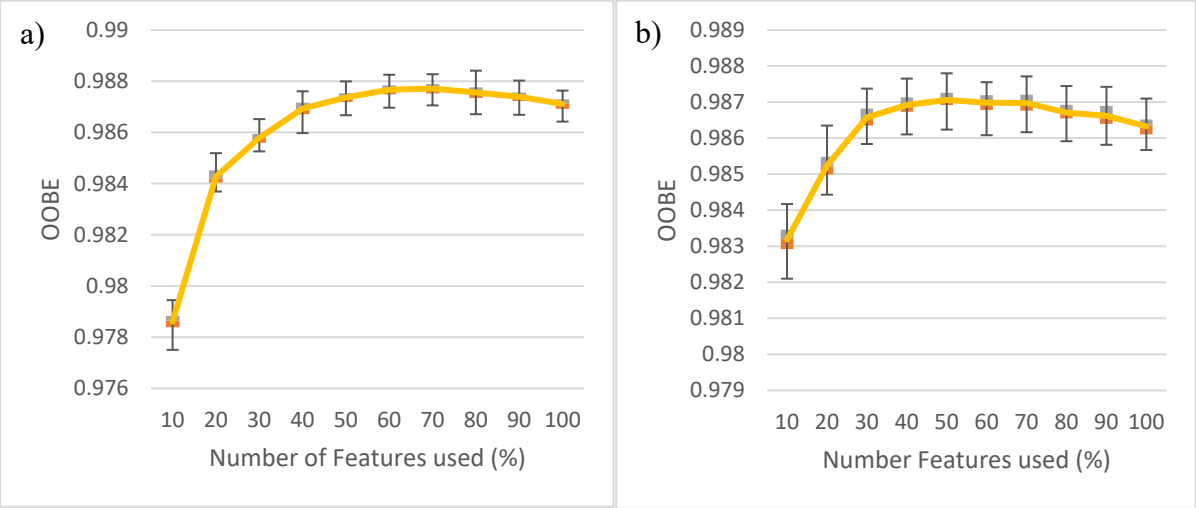

Figure 5 – Adjusting "max_features" parameter for Robinson Ridge a) 2011 and b) 2014 Random Forrest Models. 100 iterations of model were run for each setting, error bars indicate maximum/minimum values, 2011 optimal value = 70%, 2014 optimal value = 50%.

3.3 Random Forest Model cross-validation

Once the optimal parameters for the RFM have been determined, it is necessary to obtain an accurate measure of the model performance. As described in Section 2.8, we cross-validated the RFMs against all possible testing data combinations. The Robinson Ridge 2011 dataset used 20 quadrats, which provides 15504 combinations, when using 15 quadrats to train the RFM and 5 quadrats to test the model. The average RMSE of the test quadrats was found to be 12.18%. The Robinson Ridge 2014 dataset was tested in a similar manner. However, there were only 8 quadrats

available, thus 2 were used to test and 6 for training, which yielded 28 combinations. The average RMSE was found to be 7.44%.

3.4 Importance of Input Variables

Once trained, an RFM produces a report on the importance of input variables, i.e. which variable had the strongest contribution during the model training. As suggested by Millard and Richardson (2015), the variable importance measure can be used to reduce the number of input variables, whilst maintaining or even improving model accuracy. Figure 6 shows that for both the 2011 and 2014 RFMs, there are 5 variables (e.g. Refl_800, MTVI, Skyview, LN_FLowAcc, and TIR) with significantly higher importance scores than the rest of the variables. Nevertheless, reducing the number of input variables and re-training each RFM did not significantly change the RMSE (Table 2).

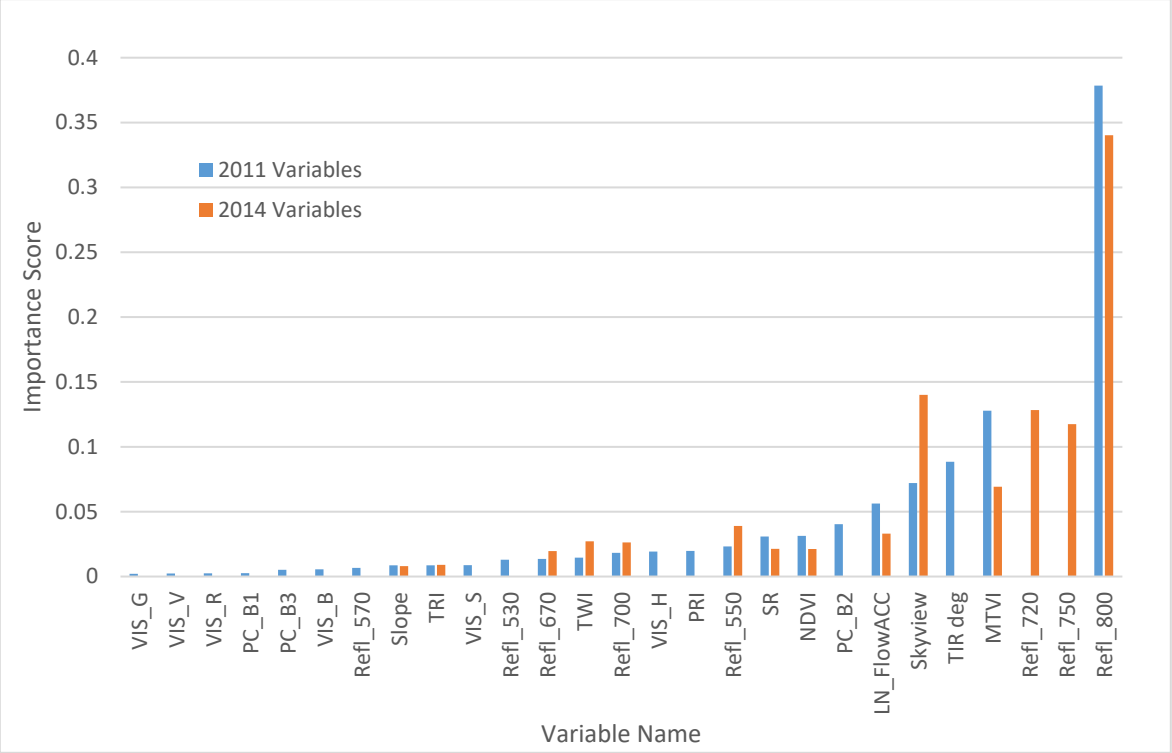

Figure 6 – Importance scores for Robinson Ridge 2011 and 2014 Random Forest Model input variables.

Table 2 – Effect of removing input variables with low importance scores.

RFM	RMSE – Using all variables	RMSE – Using only top 5 variables
Robinson Ridge 2011	12.18%	12.51%
Robinson Ridge 2014	7.44%	7.32%

The variable importance measure additionally allows us to test various combinations of input variables, more specifically, to test combinations of variables that are derived from specific sensors. This helps us to determine, if any sensor or sensors can be removed from the dataset without significant effect on the performance of the RFM (Corcoran et al. (2013). Our dataset effectively contained data from four sensors: i) the variables derived from the RGB sensor, ii) variables from the MCA sensor, iii) the variable from the TIR sensor, and iv) the terrain data derived from the RGB sensor, but treated separately. The terrain data can be considered as a constant measurement, because the terrain variables are unlikely to change significantly over time, as long as the area is clear of snow. With the four sensors we have 13 combinations to test, and for each of these combinations we ran a full cross-validation for all possible combinations of test quadrats, as described in Section 3.3. For the Robinson Ridge site in 2014, data collected by the RGB or TIR sensor were missing, resulting in fewer combinations to test. The results of these RFM runs are presented in Table 3.

Table 3 – Accuracy performance (RMSE) of Random Forest Models for different combinations of sensors.

Combination of Sensors	Robinson Ridge 2011	Robinson Ridge 2014
RGB + Terrain + MCA + TIR	12.18%	N/A
RGB only	14.01%	N/A
Terrain data only	16.85%	10.99%
MCA data only	11.64%	8.15%
RGB + Terrain	13.69%	N/A
RGB + MCA	11.22%	N/A
RGB + TIR	15.31%	N/A
MCA + TIR	12.28%	N/A
Terrain + MCA	11.61%	7.42%
Terrain + TIR	18.03%	N/A
RGB + Terrain + MCA	11.22%	N/A
RGB + Terrain + TIR	15.23%	N/A
Terrain + MCA + TIR	12.60%	N/A

3.5 Performance of the Random Forest Models

As a final accuracy assessment of the RFMs, we trained models for the Robinson Ridge 2011 and 2014 datasets with all of the quadrats observed in the respective years, i.e. no quadrats were held back for validation. Figure 7 shows how well each model performs across each of the training

datasets. The models trained with the entire dataset were considered to be the most robust and were, therefore, used to estimate moss health for the entire mapped research area.

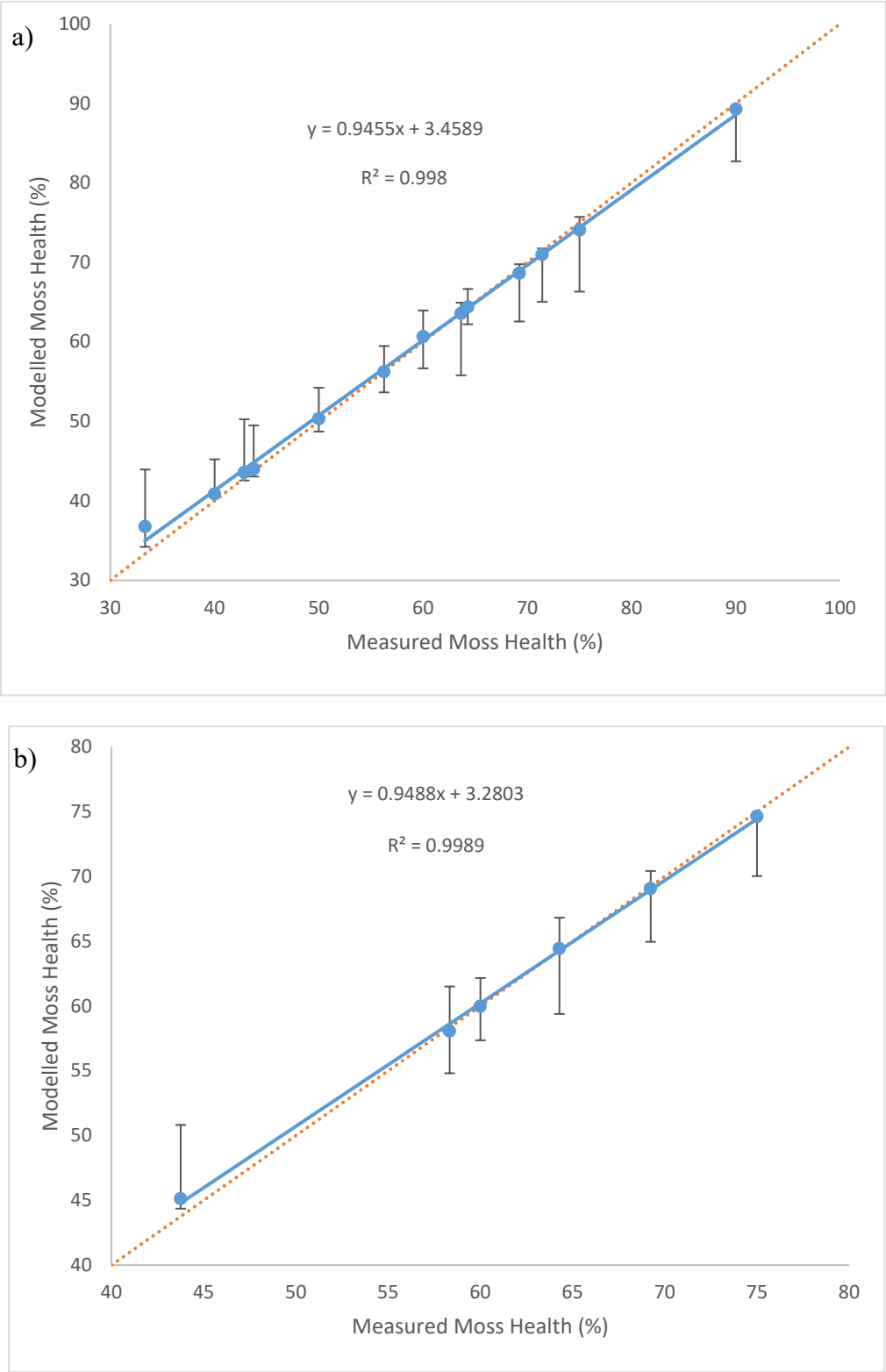

Figure 7 – Performance of Robinson Ridge a) 2011 and b) 2014 Random Forest Models (error bars show range of pixel health values within a given quadrat, orange line is one-to-one line).

3.6 Generic Random Forest Model

In sections 3.1 - 3.5 our results (see Figure 7) clearly demonstrate that an RFM can be successfully trained to estimate the spatial distribution of moss health across an entire moss bed. However, each of the models for 2011 and 2014 were trained with data from their respective years. Thus, to investigate the method transferability, we tested if a model trained on quadrat data from 2011 could be applied to data from 2014 and still produce plausible moss health thematic maps.

The already trained 2011 RFM could not be used for this purpose, as it used input variables that were not available in the 2014 dataset, thus it had to be retrained for variables common to both datasets. Table 1 highlights the 14 variables that are available in the 2014 dataset of which 12 variables are available in both datasets.

An RFM model (henceforth denoted 2011_reduced) was trained with the reduced set of input variables and the optimal parameters as found in Sections 3.1 and 3.2. A cross-validation was carried out for the 2011_reduced RFM (as detailed in Section 2.8) and the average RMSE was found to be 11.85%, a similar error to the 2011 and 2014 RFMs (see Table 2). Looking at the variable importance scores for the 2011_reduced model, a similar pattern can be observed, with the six most important input variables in descending order of importance: Refl_800, SR, NDVI, Skyview, MTVI and LN_FlowAcc. As with the other RFMs, we built the final 2011_reduced model using all available training data in order to create the most robust algorithm possible.

The accuracy of the 2011_reduced model was assessed by comparing its health predictions with the independent in situ moss health measurements carried out at the eight viable quadrats within the area mapped in 2014. The health prediction RMSE for these eight quadrats was found to be 10.7%, which is in line with the cross-validation performance of 11.85%. This level of accuracy is acceptable considering the fact that the 2011_reduced RFM had not been presented with these 2014 validation quadrats during the training phase.

3.7 Inter-seasonal moss health mapping

Using the 2011 RFM and the 2011_reduced RFM, trained with all available data, the Robinson Ridge UAS image datasets were processed to produce per-pixel thematic maps of moss health for both years 2011 and 2014, respectively. The rocks and soil were masked out by thresholding the MTVI optical index at a value of 0.1. All remaining pixels were used for RFM health prediction [%]. Figure 8 presents the health assessment maps of the most continuous moss bed section at the Robinson Ridge site in 2011 and 2014, respectively. Visually, one can see only minor changes in the

distribution of moss health between the years. When considering the investigated time span and relatively limited spatial extent, any moss health change is likely to be undetectable by the RFM algorithms with the inherent moss health prediction errors from approximately 5 to 10%. Despite the uncertainty in the 2014 RFM output, Figure 8 visually illustrates the potential for multi-source multi-temporal UAS data to be used for spatially explicit change detection at very high spatial resolution.

Figure 8 – Modelled moss health (%) for main moss bed at Robinson Ridge in (a) 2011 and (b) 2014 (coordinate reference system: UTM, zone 49 South).

Discussion

The results presented in this study demonstrate that careful testing of the RFM parameters has a significant impact on the RFM performance. In particular, the RFM performance can be improved if the number of features considered at each split is not left as the default value of all the variables, but thoroughly tested and optimised. In our study, a lower value provided more optimal model performance. Additionally, identifying the lowest number of trees, at which the Out of Bag Error has converged, revealed the optimal RFM configuration.

Although the final RMSE for the Robinson Ridge 2014 RFM estimates is lower (7.44%) compared to the estimates from 2011 (12.18%), the 2011 result is more robust as there were more useable training/testing quadrats available (20 quadrats for 2011 vs. 8 quadrats for 2014). Consequently, the

2014 RFM was trained with fewer quadrats representing a smaller range of moss health (see Figure 1 and Figure 7), whereas the 2011 RFM could use a wider and more representative range of health values present in the more extensive dataset. The 2011 RMSE of 12.18% reflects a high diversity in health values presented to the RFM during training and testing phases and could be considered as the worst error likely to be produced by the model. A significant part of this error originates from poor performance of the 2011 RFM when being validated with quadrats containing extremely low or high health values. The lowest health recorded in the Robinson Ridge field observations was a single quadrat with a health of 33%. If this quadrat is used for testing but not for training purposes, then the prediction of unhealthy moss is inaccurate and the resulting model error is large (> 20%). Such poorly performing test quadrats have a significant effect on the overall mean RMSE, but since we trained the final RFM using all available quadrats, it is unlikely that this underrepresentation was propagated in to the final moss health maps. Unfortunately, when using all the data for training, we had no independent samples to calculate an actual RMSE. We, therefore, used the OOBE, which provides a pseudo measure of the model accuracy. The underlying weakness of the 2014 results is a limited size of training dataset with only twelve quadrats, four of which were flooded with meltwater during UAS data acquisition.

Indication of the input variable significance showed that the NIR reflectance (at 800 nm) was of high importance to both the 2011 and 2014 Robinson Ridge RFMs. Variables derived from the terrain model, i.e. Skyview and Flow Accumulation, were also indicated as important for both RFMs. When all the possible combinations of available sensors were tested, it was found that the multispectral (MCA) data is present in the top performing combinations. The three best combinations, identified for 2011 RFM, are: i) MCA reflectance + RGB image + Terrain derivatives, ii) MCA bands only, and iii) MCA reflectance + Terrain derivatives. This leads to the conclusion that multispectral (or hyperspectral) reflectance data containing NIR bands is essential for health assessment of Antarctic moss beds. It is important to mention that the Tetracam MCA image data that we used in this study suffered from sensor noise, which influenced performance of the RFM.

Malenovský et al. (2015) and Malenovský et al. (2017) demonstrated that the spectral signature of healthy moss is quite different to that of stressed moss, particularly between 650 and 780 nm. These findings align with the importance of the near-infrared reflectance data as shown in Figure 6, which highlights that the 720 and 750 nm bands (around the red edge region of the spectrum) have a high variable importance score. In the 2014 dataset much of the information contained in the MTVI is captured in the extra near infrared bands (720 and 750 nm) and thus the importance of MTVI has dropped and Skyview has taken over as an important indicator of health We know from previous studies (Lucieer et al., 2014b), that there is a relationship between water availability and health. It is

likely that for the 2011 dataset, surface temperature is acting as a proxy for the moisture of the moss beds, whilst in 2014 the thermal infrared data are missing, and Skyview has a higher importance as it is likely that it is acting as a proxy for solar illumination.

Applying the RFMs to the Robinson Ridge 2011 and 2014 image mosaics of the entire research area allowed us to create thematic moss health maps of a very high spatial resolution of a quality that would be extremely useful to Environmental Managers tasked with preserving Antarctic biodiversity. A visual comparison of the two maps (Figure 8) illustrates there is very little change between the years for the largest continuous section of moss bed at the Robinson Ridge study site. This is not unexpected given the slow growth rates of Antarctic mosses (Clarke et al., 2012) and the fact that this map covers the mid-range of quadrat locations encompassing both transitional and bryophyte areas (see Figure 1). The transitional region changes less rapidly than the bryophyte areas (Robinson and King, 2017 pers. comm. 31 Oct) and the time between data collection is likely too short to enable detection of significant changes in either community (Robinson and King, 2017 pers. comm. 31 Oct). To be truly useful for spatial change detection, the RFM methodology needs to be applied to an area with a large spatial extent and over a longer period with more frequent revisits. Although these initial results illustrate a successful application of a machine learning approach based on RFMs, it is not feasible to make statistically robust conclusions about the change in moss health from a single inter-seasonal comparison. This requires additional data to be acquired during multiple seasons at more than a single study site, which would need to be supported by field observations of health change in the longer term. Additionally, the highly dynamic environmental conditions, especially local weather, may produce intra-seasonal changes in moss health (Robinson and King, 2017 pers. comm. 31 Oct). For example, the mean temperature recorded at Casey station in February 2011 and 2014 was -1.5 °C and 0.1 °C, respectively. This seemingly minor temperature change, crosses the melt threshold, resulting in different onsets and intensity of local, seasonal snowmelt, which impose significantly different levels of stress and may affect the spatial variability of healthy and unhealthy moss within and between seasons.

There are a few other studies that provide a spatially explicit approach to moss health mapping at landscape scales. The results of this study are unique in several aspects: maps of moss health were created for two growing seasons; multiple input variables from multiple sensors were used to estimate moss health; and the moss health maps were produced at a very high spatial resolution, not only detailing the extent of the moss vegetation, but also its health state.

There is, however, still more experimental work required for the robustness of the RFM technique to be validated. We demonstrated that an RFM could be trained on data collected in one season, and then applied to another season and still produce accurate moss health estimations (see Section 3.6).

What is now required is a demonstration of the transferability of this technique to another Antarctic moss study site. This will require the collection of further UAS and *in situ* validation data, however, the methodology for future data collection can be guided by the results of this study, i.e. the order of the UAS sensor deployment can be prioritised to ensure the most important input variables are collected first.

The moss beds should be mapped at a regular interval. The long-term monitoring program that collects the quadrat data revisits the sites every five years. Ideally, UAS mapping should be carried out at the same time to allow the ground sampling data to be linked and extrapolated to the entire moss bed. Regular monitoring of two other sites in the vicinity (within 10 km of Casey Station) should also be undertaken, Stevenson's lagoon and Antarctic Special Protected Area 135 (ASPA135). However, as logistical opportunities arise the mapping program should be expanded to other moss beds around the Antarctic continent.

The resolution (3 cm/pixel) of the multispectral imagery collected in this study was found to be optimal as it is sufficient for the moss to be accurately discriminated from the surrounding rocks and the flight time required to complete the mapping is within the operational abilities of most UAS airframes. When selecting the area to be mapped it is important to ensure that the topography of the moss bed catchment is captured if feasible, i.e. it is not under snow and is logistically possible. The resolution (2 cm/pixel) of the terrain model captured for this study allowed accurate modelling of important terrain derivatives such as flow accumulation and Skyview, and hence future data capture campaigns should capture imagery at an equivalent resolution.

Despite the logistical challenges of UAS data collection in Antarctica, there is currently no other remote sensing technique that can provide the high spatial and spectral resolution required to map the fragmented moss ecosystems. Very high resolution satellite imagery could be used to detect the presence of moss, but currently the spatial resolution is too restrictive to capture pure moss pixels in these fragmented communities (i.e. many mixed pixels). Also, cloud cover is prevalent in the Antarctic coastal region, which makes space borne remote sensing impractical. Future technological developments in long endurance UAS could overcome some of the current operational limitations.

This study has also provided important insight into the type of data that is most suitable for UAS-based estimation of moss health. Such knowledge is essential for making decisions about sensors that should be deployed in future monitoring campaigns, especially in remote environments such as Antarctica, with complicated logistics and limited transport capacity. Since this study, new UAS optical sensors with improved performance are available in particular multispectral and hyperspectral frame cameras, see Adão et al. (2017) for examples of current technology. Thermal

sensors have also been improved from the perspective of radiometric calibration and resolution, providing more accurate surface temperature measurements than their predecessors (Maes et al., 2017). Therefore, future UAS Antarctic campaigns, involving deployment of these modern sensors, are expected to produce data and derived biophysical properties of better quality, resulting in more accurate and robust health maps of moss beds across Antarctica, which would be valuable tools for the Environmental Managers of Antarctic Nations (Terauds and Lee, 2016).

Conclusions

This study has demonstrated the suitability of Random Forest Models (RFM) for assessment of the health status of Antarctic moss beds based on data collected with a remote sensing multi-sensor Unmanned Aircraft Systems (UAS). The use of ground based quadrats as training and testing data for the RFM enabled us to model and predict moss health with an RMSE between 7 and 12%. We have shown that coupling ground samples with ultra-high resolution UAS imagery and use of a modern machine learning algorithm, in our case RFM, allows for fast and accurate spatial prediction of field moss health observations of the entire moss bed ecosystem.

In order to achieve optimal RFM performance, some care needs to be taken when setting model parameters during the training phase. A by-product of the RFM training process is the importance indication of each input variable. We found that near infrared (NIR) moss turf reflectance is essential for our RFM moss health assessment. The most useful contributions from cameras capturing the visible part of the electromagnetic spectrum were terrain derivatives, such as skyview factor and flow accumulation, which were modelled from overlapping images.

Because of temporal and logistical constrains in collecting data in remote Antarctic locations, the combination of UAS-based remote sensing and the machine learning RFM technique provides a unique tool for monitoring moss health across a larger spatial extent. Yet, the performance of an RFM is only as good as the representativeness of training data used to create it. Thus it is essential that in future Antarctic field work, a sufficient number of ground validation sites (quadrats) are remotely sensed from a UAS. Our approach provides the possibility to detect spatial inter-seasonal changes, however, potential intra-seasonal variations and the accuracy of the RFM have to be considered before drawing any ultimate conclusions. Further research into the seasonal dynamics of moss physiology along with more UAS-based datasets acquired at multiple Antarctic locations are required to provide statistically robust change detection maps that represent general trends in the

health of Antarctic mosses. Nevertheless, the methods developed in this study established a good base for a future monitoring program based on ultra-high resolution UAS remote sensing.

Acknowledgments

This project was funded by Australian Research Council DP110101714 and Australian Antarctic Division (AAD; Australian Antarctic Science Grants 3130, 1313 and 4046, 4361). Logistic support was also provided by these AAD grants. DK would like to acknowledge funding from an Australian Postgraduate Award. We thank Jane Wasley, Johanna Turnbull for setting up the original quadrats, and ANARE expeditioners in for their field support.

References

Adão, T., Hruška, J., Pádua, L., Bessa, J., Peres, E., Morais, R., Sousa, J., 2017. Hyperspectral Imaging: A Review on UAV-Based Sensors, Data Processing and Applications for Agriculture and Forestry. Remote Sensing 9, 1110.

Akar, Ö., Güngör, O., 2015. Integrating multiple texture methods and NDVI to the Random Forest classification algorithm to detect tea and hazelnut plantation areas in northeast Turkey. International Journal of Remote Sensing 36, 442-464.

Amesbury, M.J., Roland, T.P., Royles, J., Hodgson, D.A., Convey, P., Griffiths, H., Charman, D.J., 2017. Widespread Biological Response to Rapid Warming on the Antarctic Peninsula. Current biology : CB 27, 1616-1622.e1612.

Ashcroft, M.B., Casanova-Katny, A., Mengersen, K., Rosenstiel, T.N., Turnbull, J.D., Wasley, J., Waterman, M.J., Zúñiga, G.E., Robinson, S.A., 2016. Bayesian methods for comparing species physiological and ecological response curves. Ecological Informatics 34, 35-43.

Ashcroft, M.B., King, D., Raymond, B., Turnbull, J.D., Wasley, J., Robinson, S.A., 2017. Moving beyond presence and absence when examining species range shifts. . Global Change Biology.

Bollard-Breen, B., Brooks, J.D., Jones, M.R.L., Robertson, J., Betschart, S., Kung, O., Craig Cary, S., Lee, C.K., Pointing, S.B., 2014. Application of an unmanned aerial vehicle in spatial mapping of terrestrial biology and human disturbance in the McMurdo Dry Valleys, East Antarctica. Polar Biology 38, 573-578.

Boulesteix, A.-L., Janitza, S., Kruppa, J., König, I.R., 2012. Overview of Random Forest Methodology and Practical Guidance with Emphasis on Computational Biology and Bioinformatics. WIREs Data Mining & Knowledge Discovery.

Breiman, L., 2001. Random Forests. Machine Learning 45, 5-32.

Casanovas, P., Black, M., Fretwell, P., Convey, P., 2015. Mapping lichen distribution on the Antarctic Peninsula using remote sensing, lichen spectra and photographic documentation by citizen scientists. Polar Research 34.

Clarke, L.J., Robinson, S.A., Hua, Q., Ayre, D.J., Fink., D., 2012. Radiocarbon bomb spike reveals biological effects of Antarctic climate change. Global Change Biology 18, 301-310.

Conrad, O., Bechtel, B., Bock, M., Dietrich, H., Fischer, E., Gerlitz, L., Wehberg, J., Wichmann, V., Böhner, J., 2015. System for Automated Geoscientific Analyses (SAGA) v. 2.1.4. Geosci. Model Dev. 8, 1991-2007.

Convey, P., Bindschadler, R., di Prisco, G., Fahrbach, E., Gutt, J., Hodgson, D.A., Mayewski, P.A., Summerhayes, C.P., Turner, J., Consortium, A., 2009. Antarctic climate change and the environment. Antarctic Science 21, 541-563.

Convey, P., Chown, S., Clarke, A., Barnes, D., Bokhorst, S., Cummings, V., Ducklow, H., Frati, F., Green, T., Gordon, S., Griffiths, H., Howard-Williams, C., Huiskes, A., Laybourn-Parry, J., Lyons, W., McMinn, A., Morley, S., Peck, L., Quesada, A., Robinson, S., Schiaparelli, S., Wall, D., 2014. The spatial structure of Antarctic biodiversity. Ecological Monographs 84, 203-244.

Corcoran, J., Knight, J., Gallant, A., 2013. Influence of Multi-Source and Multi-Temporal Remotely Sensed and Ancillary Data on the Accuracy of Random Forest Classification of Wetlands in Northern Minnesota. Remote Sensing 5, 3212-3238.

Dunn, J.L., Robinson, S.A., 2006. Ultraviolet B screening potential is higher in two cosmopolitan moss species than in a co-occurring Antarctic endemic moss: implications of continuing ozone depletion. Global Change Biology 12, 2282-2296.

Eisavi, V., Homayouni, S., Yazdi, A.M., Alimohammadi, A., 2015. Land cover mapping based on random forest classification of multitemporal spectral and thermal images. Environmental Monitoring and Assessment 187, 1-14.

Feng, Q., Liu, J., Gong, J., 2015. UAV Remote Sensing for Urban Vegetation Mapping Using Random Forest and Texture Analysis. Remote Sensing 7, 1074.

Gamon, J.A., Penuelas, J., Field, C.B., 1992. A narrow-waveband spectral index that tracks diurnal changes in photosynthetic efficiency. Remote Sensing of Environment 41, 35-44.

Haboudane, D., Miller, J.R., Pattey, E., Zarco-Tejada, P.J., Strachan, I.B., 2004. Hyperspectral vegetation indices and novel algorithms for predicting green lai of crop canopies: Modeling and validation in the context of precision agriculture. Remote Sensing of Environment 90, 337-352.

Hammond, T.O., Verbyla, D.L., 1996. Optimistic bias in classification accuracy assessment. International Journal of Remote Sensing 17, 1261-1266.

Immerzeel, W.W., Kraaijenbrink, P.D.A., Shea, J.M., Shrestha, A.B., Pellicciotti, F., Bierkens, M.F.P., de Jong, S.M., 2014. High-resolution monitoring of Himalayan glacier dynamics using unmanned aerial vehicles. Remote Sensing of Environment 150, 93-103.

Javernick, L., Brasington, J., Caruso, B., 2014. Modeling the topography of shallow braided rivers using Structure-from-Motion photogrammetry. Geomorphology 213, 166-182.

Lawrence, R.L., Wood, S.D., Sheley, R.L., 2006. Mapping invasive plants using hyperspectral imagery and Breiman Cutler classifications (randomForest). Remote Sensing of Environment 100, 356-362.

Liaw, A., Wiener, M., 2002. Classification and Regresssion by randomForest. R News 2, 18-22.

Lovelock, C.E., Robinson, S.A., 2002. Surface reflectance properties of Antarctic moss and their relationship to plant species, pigment composition and photosynthetic function. Plant, Cell & Environment 25, 1239-1250.

Lucieer, A., Malenovský, Z., Veness, T., Wallace, L., 2014a. HyperUAS-Imaging Spectroscopy from a Multirotor Unmanned Aircraft System. Journal of Field Robotics.

Lucieer, A., Robinson, S., Turner, D., 2011. Unmanned Aerial Vehicle (UAV) Remote Sensing for Hyperspatial Terrain Mapping of Antarctic Moss Beds based on Structure from Motion (SfM) point

clouds, 34th International Symposium for Remote Sensing of the Environment (ISRSE), Sydney Australia.

Lucieer, A., Robinson, S., Turner, D., Harwin, S., Kelcey, J., 2012. Using a micro-UAV for ultra-high resolution multi-sensor observations of Antarctic moss beds, International Archives of the Photogrammetry, Remote Sensing and Spatial Information Sciences - ISPRS Archives, pp. 429-433.

Lucieer, A., Turner, D., King, D.H., Robinson, S.A., 2014b. Using an Unmanned Aerial Vehicle (UAV) to capture micro-topography of Antarctic moss beds. International Journal of Applied Earth Observation and Geoinformation 27, 53-62.

Maes, W., Huete, A., Steppe, K., 2017. Optimizing the Processing of UAV-Based Thermal Imagery. Remote Sensing 9, 476.

Malenovský, Z., Lucieer, A., King, D.H., Turnbull, J.D., Robinson, S.A., 2017. Unmanned aircraft system advances health mapping of fragile polar vegetation. Methods in Ecology and Evolution, 1-15.

Malenovský, Z., Turnbull, J., Lucieer, A., Robinson, S., 2015. Antarctic moss stress assessment based on chlorophyll content and leaf density retrieved from imaging spectroscopy data. . New Phytologist 208, 608-624.

Melick, D.R., Hovenden, M.J., Seppelt, R.D., 1994. Phytogeography of bryophyte and lichen vegetation in the Windmill Islands, Wilkes Land, Continental Antarctica. Vegetatio 111, 71-87.

Millard, K., Richardson, M., 2015. On the Importance of Training Data Sample Selection in Random Forest Image Classification: A Case Study in Peatland Ecosystem Mapping. Remote Sensing 7, 8489-8515.

Robinson, S.A., King, D.H., 2017. Pers. Comm. 31 Oct.

Robinson, S.A., Wasley, J., Tobin, A.K., 2003. Living on the edge–plants and global change in continental and maritime Antarctica. Global Change Biology 9, 1681-1717.

Smith, G.M., Milton, E.J., 1999. The use of the empirical line method to calibrate remotely sensed data to reflectance. International Journal of Remote Sensing 20, 2653-2662.

Smith, R.I.L., 1988. Classification and Ordination of Cryptogamic Communities in Wilkes Land, Continental Antarctica. Vegetatio 76, 155-166.

Sørensen, R., Zinko, U., Seibert, J., 2006. On the calculation of the topographic wetness index: evaluation of different methods based on field observations. Hydrol. Earth Syst. Sci. 10, 101-112.

Stumpf, A., Kerle, N., 2011. Combining Random Forests and object-oriented analysis for landslide mapping from very high resolution imagery. Procedia Environmental Sciences 3, 123-129.

Terauds, A., Lee, J.R., 2016. Antarctic biogeography revisited: updating the Antarctic Conservation Biogeographic Regions. Diversity and Distributions 22, 836-840.

Tucker, C.J., 1979. Red and photographic infrared linear combinations for monitoring vegetation. Remote sensing of Environment 8, 127-150.

Turnbull, J.D., Robinson, S.A., 2009. Accumulation of DNA damage in Antarctic mosses: correlations with ultraviolet-B radiation, temperature and turf water content vary among species. Global Change Biology 15, 319-329.

Turner, D., Lucieer, A., Malenovský, Z., King, D., Robinson, S., 2014a. Spatial Co-Registration of Ultra-High Resolution Visible, Multispectral and Thermal Images Acquired with a Micro-UAV over Antarctic Moss Beds. Remote Sensing 6, 4003-4024.

Turner, D., Lucieer, A., Wallace, L., 2014b. Direct Georeferencing of Ultrahigh-Resolution UAV Imagery. IEEE Transactions on Geoscience and Remote Sensing 52, 2738-2745.

Turner, D., Lucieer, A., Watson, C., 2012. An Automated Technique for Generating Georectified Mosaics from Ultra-High Resolution Unmanned Aerial Vehicle (UAV) Imagery, Based on Structure from Motion (SfM) Point Clouds. Remote Sensing 4, 1392-1410.

Verhoeven, G., 2011. Taking computer vision aloft - archaeological three-dimensional reconstructions from aerial photographs with photoscan. Archaeological Prospection 18, 67-73.

Wang, L.a., Zhou, X., Zhu, X., Dong, Z., Guo, W., 2016. Estimation of biomass in wheat using random forest regression algorithm and remote sensing data. The Crop Journal 4, 212-219.

Wasley, J., Robinson, S.A., Turnbull, J.D., King, D.H., Wanek, W., Popp, M., 2012. Bryophyte species composition over moisture gradients in the Windmill Islands, East Antarctica: development of a baseline for monitoring climate change impacts. Biodiversity 1, 257-264.

Yuan, Y., Hu, X., 2016. Random Forest and Objected-Based Classification for Forest Pest Extraction from UAV Aerial Imagery. Int. Arch. Photogramm. Remote Sens. Spatial Inf. Sci. XLI-B1, 1093-1098.

Zhu, X., 2013. Land cover classification using moderate resolution satellite imagery and random forests with post-hoc smoothing. Journal of Spatial Science 58, 323-337.